Vibrationally mediated transport in molecular transistors

D. H. Santamore,[1,2,*] Neill Lambert,[2] and Franco Nori[2,3]

[1]*Department of Physics, Temple University, Philadelphia, Pennsylvania 19122, USA*
[2]*Advanced Science Institute, RIKEN, Saitama 351-0198, Japan*
[3]*Physics Department, University of Michigan, Ann Arbor, Michigan 48109, USA*

We investigate the steady-state electronic transport through a suspended dimer molecule coupled to leads. When strongly coupled to a vibrational mode, the electron transport is enhanced at the phonon resonant frequency and higher order resonances. The temperature and bias determine the nature of the phonon-assisted resonances, with clear absorption and emission peaks. The strong coupling also induces a Frank-Condon-like blockade, suppressing the current between the resonances. We compare an analytical polaron transformation method to two exact numerical methods: the Hierarchy equations of motion and an exact diagonalization in the Fock basis. In the steady state, our two numerical results are an exact match and qualitatively reflect the main features of the polaron treatment. Our results indicate the possibility of a new type of molecular transistor or sensor where the current can be extremely sensitive to small changes in the energies of the electronic states in the dimer.

I. INTRODUCTION

Electron transport through real, and artificial, suspended molecular systems has revealed a rich tapestry of physical effects.[1–8] Nanomechanical systems offer the promise of observing quantum effects in massive objects,[9–11] which can be cooled, driven, measured, and manipulated using electron transport.[7,12–21] Single-molecule electronics offers similar promises, with the benefit of stronger coupling of vibrational and oscillatory modes to the transport process and a large range of practical applications.[22–34] Current efforts on single-molecule electronics include the exploration of the electronic level structure and its effect on electronic transport together with the development of electronic devices and applications.[35]

Since the performance of molecular electronic devices depends on electron transfer between molecules, it ultimately requires a good understanding of coherent transport and dynamics. Molecular electronics has a variety of predecessors in chemistry and chemical reactions, known as electron-transfer reactions.[36,37] One particular example, the donor-bridge-acceptor (DBA) system, has been studied for a long time and used to probe the mechanisms of charge transfer.[38] In this system, the donor molecule donates an electron to the acceptor via the third nonrigid or rigid molecule called a "bridge" (i.e., redox reaction). In the laboratory it is possible to construct a molecular electronics device by attaching electrodes to the donor and acceptor molecules of a mixed-valence dimer and apply a bias voltage to cause electron transport. Aviram and Ratner[39] made the first metal-DBA-metal system in analogy to p-n junctions. The transfer rate of incoherent transfer can be explained within the well-known Förster and Dexter theory,[40–43] and until recently, coherent transport had been regarded to play only a small role in charge-transfer dynamics of molecules. However, this view has been changed in the last decade and some experiments indicate that coherent transport is indeed important.[44,45]

In a slightly different context, recent experiments in photosynthetic complexes have shown that *excitonic* coherence lasts surprisingly long at nonzero temperatures: up to 300 fs at room temperature.[46–48] It has recently been proposed[49,50] that

the vibrational modes in the protein environment may also play a role in the observed oscillations, long coherence time, and high transport efficiency. Therefore, an understanding of the intricacies of both coherent electron transport and coherent exciton transport transport in molecules, coupled to vibrational modes, is vital.[38,46,51–57]

In this paper, we examine a model of electron transport through a two-site system coupled linearly to a single vibrational mode. Motivated by recent progress in single-molecule experiments, we study the case where the electron-phonon coupling can be strong (non-perturbative) and where the phonons can have a lifetime much longer than the electronic transport process. Throughout we use the language of a single mixed-valence dimer molecule coupled to electronic leads. One electrode (source) is attached to one site of a dimer molecule (donor) and another electrode (drain) is attached to the other site (acceptor). This system is analogous to the DBA system, but instead of incoherent transport, we include the possibility of coherent electron transport and analyze steady-state dynamics and current-noise power spectra.

We begin with a semianalytical treatment based on a polaron transform, analogous to a single-mode version of the traditional "noninteracting blip approximation"(NIBA),[58,59] which can give us some insight on a regime not easily accessible with numerical methods (nonequilibrium transport, undamped vibrational mode, and strong coupling). Such an approach has been used elsewhere to study the transport through single and double quantum dots,[13,14,60,61] photosynthetic complexes[62] (and similar, though slightly different, techniques were used in),[49,50,63] and molecules. Our derivation follows in the same vein as these earlier works. We follow this with two exact numerical treatments, one based on the hierarchical equations of motion[64,65] with a Lorentz bath; the other, an exact diagonalization of the Hamiltonian in the Fock basis.

Using these various methods we show that under certain conditions the vibrational mode coupling can strongly enhance electron transport in a selective manner, suggesting the possibility of using vibrationally assisted electronic transitions as a highly sensitive transistor.

II. HAMILTONIAN

Consider a dimer molecule [denoted henceforth the left (L) and right (R) sites] with each site coupled to a lead (fermionic reservoir) so that the dimer functions as a bridge. A vibrational mode, e.g., a flexural or dilational mode of the molecule (or bridge in the D-B-A system), is coupled to the electrons in the left and right sites of the dimer. The idea of strong coupling to one vibrational mode is not far-fetched:[33,61] Such coupling has been shown experimentally in some nano–electronics devices.[66–70]

The Hamiltonian of this system, which is analogous to the Hubbard-Peierls model in the large on-site repulsion limit and with spin suppressed, can be written as

$$H = H_0 + H_T + H_V,$$

where

$$
\begin{aligned}
H_0 &= H_{\text{mol}} + H_{\text{osc}} + H_{\text{leads}}, \\
H_T &= H_{\text{tunn}} + H_{\text{couple}}, \quad (1) \\
H_V &= V_L a_L^\dagger d_S + V_R d_D^\dagger a_R + V_L d_S^\dagger a_L + V_R a_R^\dagger d_D, \quad (2)
\end{aligned}
$$

$$H_{\text{mol}} = \tfrac{1}{2}\varepsilon_L a_L^\dagger a_L + \tfrac{1}{2}\varepsilon_R a_R^\dagger a_R, \quad (3)$$

$$H_{\text{osc}} = \hbar\omega_m b^\dagger b, \quad (4)$$

$$H_{\text{leads}} = \sum_k \left(\hbar\omega_k^S d_{s,k}^\dagger d_{s,k} + \hbar\omega_k^D d_{D,k}^\dagger d_{D,k}\right), \quad (5)$$

$$H_{\text{tunn}} = T_c(a_L^\dagger a_R + a_R^\dagger a_L), \quad (6)$$

$$H_{\text{couple}} = g_L(b^\dagger + b)a_L^\dagger a_L - g_R(b^\dagger + b)a_R^\dagger a_R. \quad (7)$$

Here H_0 is the free Hamiltonian of the dimer H_{mol}, the oscillator H_{osc}, and the source and drain reservoirs H_{leads} attached to the left (right) sites, with resonant frequencies ω_L, ω_R, ω_m, ω_k^S, and ω_k^D, respectively. Also, T_c is the transmission coefficient, and $g_{L(R)}$ is the electron-vibrational-mode coupling coefficient. The annihilation (creation) operators for the electron in the molecules are $a_{L(R)}(a_{L(R)}^\dagger)$; for the lead reservoirs, $a_{S(D)}(a_{S(D)}^\dagger)$; and for the oscillator, $b(b^\dagger)$. The interaction Hamiltonian has three parts: the lead electrode-molecule coupling H_V, electron tunneling between the two sites in the dimer molecule H_{tunn}, and linear coupling between the dimer and the vibrational mode H_{couple}. The coupling between the electrons and the vibrational mode effectively modifies the frequency of the electrons on the left and right sites of the molecule as $\omega_{L(R)} \to \omega_{L(R)}^{\text{eff}}$, where $\omega_{L(R)}^{\text{eff}} = \omega_{L(R)} + g_{L(R)}(b^\dagger + b)$, while the tunneling barrier is unaffected by the coupling.

Here, for brevity, we adopt the notation

$$s \equiv a_L^\dagger a_R \quad \text{and} \quad s^\dagger \equiv a_R^\dagger a_L. \quad (8)$$

In the limit of large Coulomb repulsion to double occupation (a term not explicitly included in the Hamiltonian for simplicity), only a single electron occupies the entire molecule dimer at once. For the moment, we retain the notation for the general case, but soon we will explicitly use this assumption.

The above Hamiltonian is the most general and exact form. To find quasianalytical results, this Hamiltonian can be transformed using the polaron transformation to eliminate the interaction term, but it in turn modifies the tunneling term H_T,

$$H_T = T_c(s^\dagger X^\dagger + s X), \quad (9)$$

where

$$X \equiv \exp[z(\hat{b} - \hat{b}^\dagger)], \quad (10)$$

$$X^\dagger \equiv \exp[-z(\hat{b} - \hat{b}^\dagger),] \quad (11)$$

with $z = g/\omega_m$, $g = g_L = g_R$. Note that we have ignored a constant energy shift induced by this transformation.

The dynamics of the system can be analyzed through the master equation, where the coherent electron transport through the molecules is associated with the off-diagonal operators s, $s^\dagger$. In the next section we explicitly give details of the master equation.

III. MASTER EQUATION

To obtain the master equation, we switch to the interaction picture. In this picture $a_L^\dagger a_L$ and $a_R^\dagger a_R$ are unchanged since they commute with the noninteracting Hamiltonian:

$$a_L^\dagger a_L(t) = n_L(t) = n_L, \quad (12)$$

$$a_R^\dagger a_R(t) = n_R(t) = n_R. \quad (13)$$

For the term H_T, we define new operators that group the electron tunneling terms and vibrational mode operators,

$$\tilde{s}(t) = p \exp(i\epsilon t) X_t, \quad (14)$$

$$\tilde{s}^\dagger(t) = p^\dagger \exp(-i\epsilon t) X_t^\dagger, \quad (15)$$

where $\epsilon \equiv \epsilon_L - \epsilon_R$. Then

$$H_T(t) = T_c[\tilde{s}(t) + \tilde{s}^\dagger(t)]. \quad (16)$$

In the interaction picture, the equation of motion is

$$
\begin{aligned}
\frac{d\rho(t)}{dt} &= -\frac{i}{\hbar}[H_{\text{int}}(t), \rho(t)] \\
&= -\frac{i}{\hbar}[H_T(t) + H_V(t), \rho(t)], \quad (17)
\end{aligned}
$$

and the density matrix can be obtained by iterations. By keeping terms to second order in the couplings to the the source and drain, and making the standard Born-Markov approximation, the density matrix $\rho(t)$ can be approximated as $\rho(t) \simeq \rho_0^{DO}(t) \otimes \rho_0^{\text{res}}$. Then, after tracing out the leads, the master equation can be written in the Lindblad form,

$$
\begin{aligned}
\frac{d\rho^{DO}(t)}{dt} &= -\frac{i}{\hbar}[H_T(t), \rho^{DO}] \\
&\quad + \frac{\Gamma_L}{2}(1 - f_S)\mathcal{D}[a_L^\dagger] + \frac{\Gamma_L}{2}f_S\mathcal{D}[a_L] \\
&\quad + \frac{\Gamma_R}{2}(1 - f_D)\mathcal{D}[a_R^\dagger] + \frac{\Gamma_R}{2}f_D\mathcal{D}[a_R], \quad (18)
\end{aligned}
$$

where

$$\mathcal{D}[a_i^\dagger] \equiv a_i^\dagger a_i \rho^{DO}(t) - 2a_i \rho^{DO}(t) a_i^\dagger + \rho^{DO}(t) a_i^\dagger a_i, \quad (19)$$

$$\mathcal{D}[a_i] \equiv a_i a_i^\dagger \rho^{DO}(t) - 2a_i^\dagger \rho^{DO}(t) a_i + \rho^{DO}(t) a_i a_i^\dagger, \quad (20)$$

and f_S and f_D are the Fermi distribution functions for the left and right reservoirs, respectively, $f_S = [e^{\hbar\beta(\epsilon_L - \mu_L)} + 1]^{-1}$,

and $f_D = [e^{\hbar\beta(\epsilon_R - \mu_R)} + 1]^{-1}$. In all the subsequent results we choose an infinite bias so that $f_s = 1$, $f_d = 0$. Since we are interested in the strong-coupling limit, one may also argue that the perturbative coupling to the leads should be derived after diagonalization of the combined electronic/vibrational system. This is an interesting avenue for future work.

IV. EXPECTATION VALUES

At this point the molecule-vibrational mode coupling is still described exactly. To achieve an analytical solution it is convenient to rewrite the master equation as a closed set of equations for the expectation values of the various molecule operators, following the formulation used by Brandes[61] to describe quantum dots coupled to a bath of oscillators. To do so we need the following commutators:

$$[n_L(t), H_T(t')] = T_c[\tilde{s}(t) - \tilde{s}^\dagger(t)], \tag{21}$$

$$[\tilde{s}(t), H_T(t')] = T_c e^{i\epsilon(t-t')}\{n_L X_{t'}^\dagger X_t - n_R X_{t'}^\dagger X_t\}, \tag{22}$$

$$[\tilde{s}^\dagger(t), H_T(t')] = T_c e^{i\epsilon(t-t')}\{n_R X_{t'} X_t^\dagger - n_L X_{t'} X_t^\dagger\}. \tag{23}$$

Using these we write the following coupled integral equations for the expectation values of $\hat{n}_L, \hat{n}_R, \tilde{s}, \tilde{s}^\dagger$:

$$\langle \hat{n}_L \rangle_t - \langle \hat{n}_L \rangle_0 = -\frac{i}{\hbar}\int_0^t dt'[T_c(\langle \tilde{s}(t)\rangle - \langle \tilde{s}^\dagger(t)\rangle) + \Gamma_L \langle n_L \rangle - \Gamma_L f_S], \tag{24}$$

$$\langle \hat{n}_R \rangle_t - \langle \hat{n}_R \rangle_0 = \frac{i}{\hbar}\int_0^t dt'[T_c(\langle \tilde{s}(t)\rangle - \langle \tilde{s}^\dagger(t)\rangle) + \Gamma_R \langle n_R \rangle - \Gamma_R f_D], \tag{25}$$

$$\langle \tilde{s} \rangle_t - \langle \tilde{s} \rangle_0 = -\frac{i}{\hbar}\int_0^t dt' e^{i\epsilon(t-t')}T_c$$
$$\times \{\langle n_L X_t X_{t'}^\dagger \rangle_{t'} - \langle n_R X_{t'}^\dagger X_t \rangle_{t'}\}$$
$$+ \frac{(\Gamma_L + \Gamma_R)}{2}\int_0^t dt' e^{i\epsilon(t-t')}\langle \tilde{s}(t') X_{t'}^\dagger X_t \rangle, \tag{26}$$

$$\langle \tilde{s}^\dagger \rangle_t - \langle \tilde{s}^\dagger \rangle_0 = -\frac{i}{\hbar}\int_0^t dt' e^{-i\epsilon(t-t')}T_c$$
$$\times \{\langle n_R X_t^\dagger X_{t'} \rangle - \langle n_L X_{t'} X_t^\dagger \rangle\}$$
$$+ \frac{(\Gamma_L + \Gamma_R)}{2}\int_0^t dt' e^{-i\epsilon(t-t')}\langle X_{t'} X_t^\dagger \tilde{s}^\dagger(t')\rangle. \tag{27}$$

This is still exact, but intractable. To make progress one assumes that the molecule operators and the oscillator ones are separable, so $\langle n_L X_t X_{t'}^\dagger \rangle_{t'}$ can be written as

$$\langle n_L X_t X_{t'}^\dagger \rangle_{t'} = \langle n_L \rangle (1 - e^{-\beta\omega_B})\langle e^{-n\beta\omega_B} X_t X_{t'}^\dagger \rangle$$
$$\equiv \langle n_L \rangle \mathcal{F}, \tag{28}$$

with $\beta = k_B T$. We have also assumed that the vibrational mode is in equilibrium due to contact with the thermal bath at temperature T. The other properties of the mode are ensconced in the two-time boson correlation functions $\mathcal{F}$. In Appendix A we give an analytical form for $\mathcal{F}$ in the limit of an undamped single mode. Then one can, in principle, solve the above equations of motion for an arbitrary molecule-vibron coupling

strength (which includes non-Markovian properties of this interaction).

The polaron transformation method is powerful in that it allows us to gain simple analytical forms in some cases, and in general "plug-in" arbitrary bath correlation functions for $\mathcal{F}$, although we need to be mindful of the regime where the method is valid. Some works specify that it gives qualitatively correct results for small T_c, while a comparison to the NIBA[58] suggests that it is very accurate for $\epsilon = 0$ or $\epsilon \gg T_c, g$. For the case of a single mode, which we consider here, understanding when the results are accurate can be challenging, as we discuss in the next section. Generally, we do find them to be qualitatively correct, though additional back-action effects arise in the exact numerical treatments.

Finally, before showing explicit results, we make an additional assumption. The above equations allow for double-electron occupation of the dimer molecule. Allowing such occupation is interesting but prevents us from obtaining analytical results. Thus, as mentioned earlier, we impose another condition equivalent to the notion of Coulomb blockade in quantum dots. This is valid if the molecule is small and the bias not too large (i.e., this Coulomb repulsion is the largest energy scale). In this case only one electron can inhabit the dimer at a time and sequential tunneling occurs.

Rather than explicitly including this effect with a nonlinear repulsion against double-site occupation in the Hamiltonian, we can simply replace the fermionic operators with projectors onto the single-electron states,

$$n_L = |L\rangle\langle L|, \quad n_R = |R\rangle\langle R|, \tag{29}$$

with

$$n_L + n_R + |0\rangle\langle 0| = 1, \tag{30}$$

where $|0\rangle\langle 0|$ is the no-electron state. Similarly, $s = |L\rangle\langle R|$, $s^\dagger = |R\rangle\langle L|$. The combinations of operators in the Lindblad terms describing the coupling to the leads and Eqs. [(24)–(27)] are subtly altered by this change, to preserve the reduced Hilbert space. We do not give explicit details here, as the derivation is equivalent to the previously studied model of a double quantum dot coupled to a phonon bath,[61,71] except where the single-mode-correlation function is replaced by the spectral function for a particular bath model. For completeness we give the altered equations of motion in Appendix B. It is these equations of motion, under this additional assumption, which give us the results in the next section.

V. RESULTS

A. Current

The expectation value of the current from the source to the left molecule is $I_L(t) = -e\Gamma_L(1 - f_S)\langle n_L \rangle$, that from the right molecule to the drain is $I_R(t) = -e\Gamma_R(1 - f_D)\langle n_R \rangle$, and that from the left molecule to the right molecule is $I_L(t) = -eT_c(\langle \tilde{s}(t)\rangle - \langle \tilde{s}^\dagger(t)\rangle)$. In the steady state these three currents are the same and can easily be evaluated from the expectation values of the molecule operators described above.

The most straightforward method to solve such equations is to explicitly Laplace transform the equations of motion first and then find the coefficient of the Laplace parameter $1/z$ as $z \to 0$ in the Laurent expansion of the expectation values.[71] We
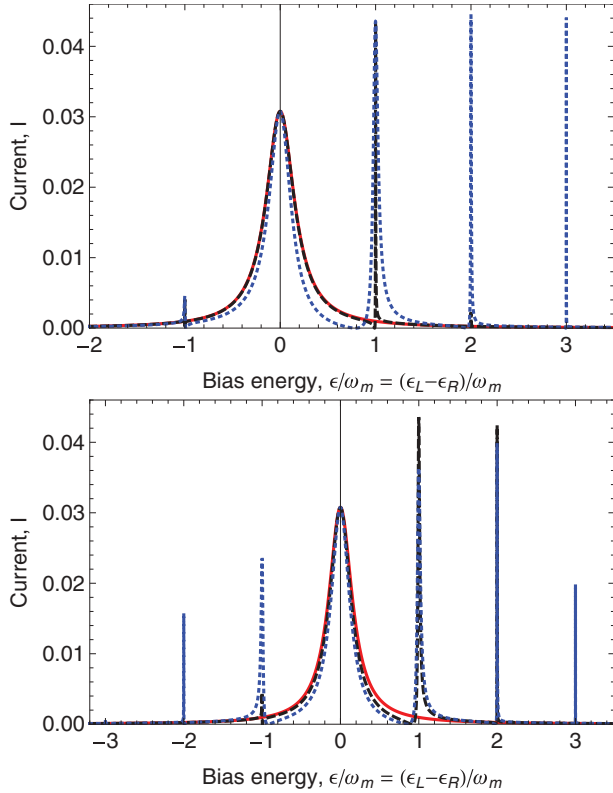
FIG. 1. (Color online) (Top) The current I_R/e, as given by the polaron transformed results, through the molecule as a function of the molecular energy bias $\epsilon/\omega_m = (\epsilon_L - \epsilon_R)/\omega_m$. The solid (red) line represents the uncoupled case, while the dashed lines are for different magnitudes of the coupling to the vibrational mode: $z = g/\omega_m$ [$z = 0.1$, long-dashed (black) line; $z = 0.5$, short-dashed (blue) line, with a thermal occupation of the vibrational mode of $N = 0.05$]. Under this polaron transformation assumption, and for a completely undamped vibrational mode, we see extremely strong vibrational emission resonances in the current. (Bottom) The current I_R/e for no coupling [solid (red) line], for coupling $z = g/\omega_m = 0.3$, and for several choices of the thermal occupation of the vibrational mode [$N = 0.01$, long-dashed (black) line; $N = 1$, short-dashed (blue) line]. As we raise the thermal temperature of the mode, absorption resonances occur, and the linewidth of the emission resonances becomes broadened. In both plots we set $\Gamma_L = \Gamma_R = 0.1$, $T_c = 0.1$, and $\omega_m = 1$.

can also use the full z-dependent forms to find the current-noise spectrum, as outlined in Sec. V B. As an example, we explicitly solve here for the current using the $\mathcal{F}$ function described in Appendix A. As discussed earlier, this allows us to investigate the unusual limit of strong coupling of the transport process to an undamped single mode. Note that, in all of the following results, we set $\hbar = 1$, $e = 1$, and typically $\omega_m = 1$, except in the noise power results.

The top plot in Fig. 1 shows the current as a function of the energy difference between the left and the right molecules (scaled with the resonant frequency of the vibrational mode) for various vibrational mode coupling strengths [$z = 0.1$, long-dashed (black) line; $z = 0.5$, short-dashed (blue) line] and without the mode coupling [solid (red) line] with a thermal occupation of the vibrational mode of $N = 0.05$. The bottom plot in Fig. 1 shows the current for different temperatures
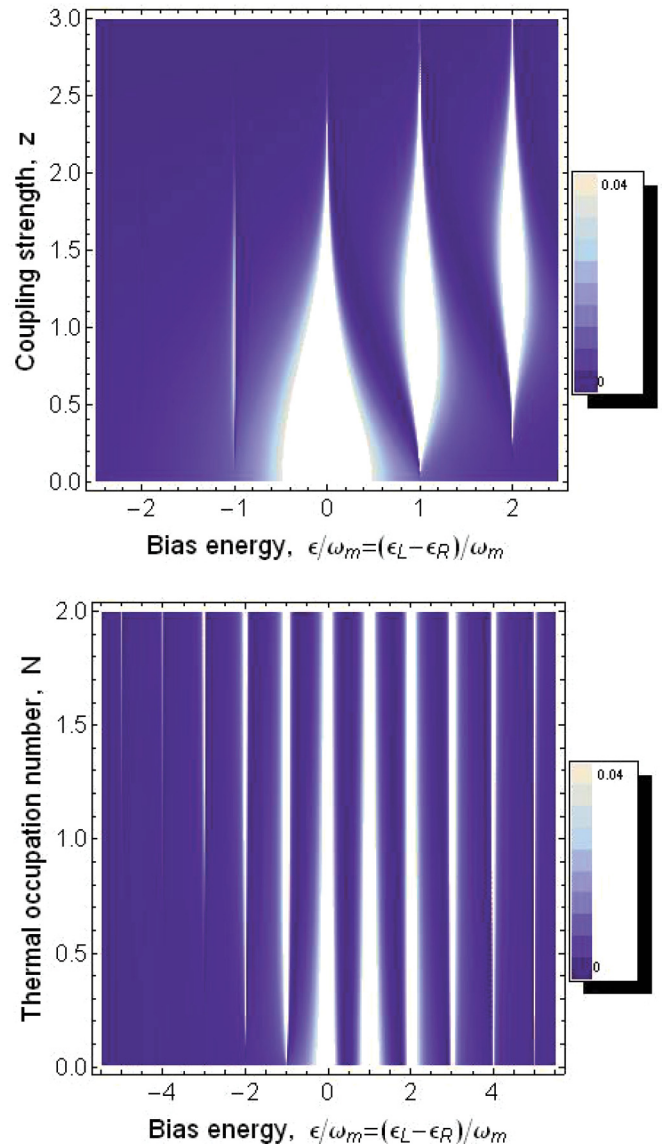

FIG. 2. (Color online) (Top) The current I_R/e through the molecule as a function of the molecular energy bias ϵ/ω_m and vibronic coupling strength $z = g/\omega_m$, with thermal occupation $N = 0.05$. (Bottom) The current I_R/e for coupling $z = g/\omega_m = 1$ as a function of ϵ and thermal occupation N. In both plots, white indicates a large current and purple represents zero current, and these results are from the polaron treatment and, again, for $\Gamma_L = \Gamma_R = 0.1$, $T_c = 0.1$, $\omega_m = 1$.

($N = 0.01$, long-dashed (black) line; $N = 1$, short-dashed (blue) line] while keeping the coupling strength constant at $z = 0.3$.

When ϵ is much larger than the tunnel coupling, the electrons cannot tunnel between the left and the right molecules and the current approaches 0. With the vibrational mode coupling "on", the current peaks when the energy bias ϵ equals the vibrational mode resonant frequency and its multiples (as also observed in the case of quantum dots coupled to a single-phonon mode).[13] Positive ϵ spikes correspond to phonon-emission-assisted transport and negative ϵ spikes correspond to phonon absorption. In Fig. 2 we see that increasing the coupling strength narrows the lower emission

peaks and broadens the higher peaks. The bottom plot in Fig. 2 shows how raising the temperature broadens and raises the absorption peaks. In addition, between peaks there is a strong suppression of the current, akin to the Franck-Condon blockade. If we directly observe, around the first resonance, the steady-state occupations of the various states, we find that this blockade effect strongly localizes the electrons in the left molecule.

The amplitudes of the absorption peaks strongly depend on the temperature. Expanding the expression for the current around the first absorption resonance, we find

$$I_{max}^{abs} = \left(\Gamma_L^{-1} + \frac{\Gamma_R}{4T_c^2} + \frac{1+2N}{\Gamma_R(1+N)} \right)^{-1}. \quad (31)$$

In contrast, the height of the emission peaks is only weakly dependent on the thermal occupation, and exactly at the resonant point, the maximum is not dependent on the coupling strength or the order, $\epsilon = n\omega$, of the resonance. For low temperatures the height of the resonance is proportional to the zero-bias current:

$$I_{max}^{emi} = I_{\epsilon=0}(1 + I_{\epsilon=0}), \quad (32)$$

$$I_{\epsilon=0} = \frac{4T_c^2}{\Gamma_R + 4T_c^2(2\Gamma_R^{-1} + \Gamma_L^{-1})}. \quad (33)$$

However, the width around the resonance is strongly dependent on both the coupling strength and the order $n\omega$ of the resonance peak. In addition, the properties of each resonance peak are almost entirely defined by the appropriate term retained in the sum in Eq. (50). Thus, overall, we can say that in between resonances there is a strong suppression of the current due to the strong coupling to the vibrational mode, and exactly on resonance (for emission) the transport channel is completely transparent. This represents a unique kind of vibrationally mediated transistor, where the transport can be exquisitely sensitive to small changes in the energies of the electronic states in the dimer.

The fact that the height of the peaks is independent of the coupling strength is surprising. Under exactly what regime are these results valid? Recall that we made two approximations in the derivation; we assumed that the electronic and bosonic operators were separable and that the bosonic correlation functions were entirely described by their thermal equilibrium state, so that

$$\langle n_L X_t X_{t'}^\dagger \rangle_{t'} = \langle n_L \rangle (1 - e^{-\beta\omega_B}) \langle e^{-n\beta\omega_B} X_t X_{t'}^\dagger \rangle. \quad (34)$$

This implies a neglect of the back-action onto the single-mode dynamics. In addition, we assumed that the dynamics of the bosonic system were not damped (though this can be included via numerical evaluations of the correlation function). These two approximations can be interpreted in the following way: that we have coupled the electron transport to a semi*classical* oscillator that is capable of emitting and absorbing energy at very specific frequencies. The fact that we neglect back-action does indicate that a quantitative difference should arise from the exact solution. In the final section we compare these results to two exact numerical models. In addition, as mentioned earlier, the set of approximations made here is, at least in the many-mode case, formally equivalent to the noninteracting blip approximation.[58,59]

B. Noise spectrum

The current-noise power spectral density is a useful and easy way, with this formalism, to gain some insight into the transient dynamics. The current-noise power has three components: particle currents through the left molecule $S_L(\omega)$, those through the right molecule $S_R(\omega)$ and the charge-noise spectrum $S_{CN}(\omega)$:[72]

$$S(\omega) = \alpha^2 S_L(\omega) + \beta^2 S_R(\omega) - \alpha\beta\omega^2 S_{CN}(\omega). \quad (35)$$

The coefficients α and β, with $\alpha + \beta = 1$, depend on the capacitances between junctions and the molecule. Here we focus on the contribution from the right particle current, which can dominate if $\beta \gg \alpha$. This contribution can be obtained from the MacDonald formula[72,73] and

$$\begin{aligned} S_R(\omega) &= 2\omega e^2 \int_0^\infty dt \sin(\omega t) \frac{d}{dt}[\langle n^2(t) \rangle - (t\langle I \rangle^2)] \\ &= 2eI\{\mathcal{L}\langle \hat{n}_i(t), \hat{n}_j(t+\tau)_{i\omega} \rangle \\ &\quad + \mathcal{L}\langle \hat{n}_i(t), \hat{n}_j(t+\tau) \rangle_{-i\omega}\}. \end{aligned} \quad (36)$$

The steady state of $S_R(\omega)$ can be calculated as

$$S_R(\omega) = 2eI\{1 + \Gamma_R[\hat{n}_R(-i\omega) + \hat{n}_R(i\omega)]\}. \quad (37)$$

The frequency-dependent $\hat{n}_R(i\omega)$ is again easily extracted from the Laplace transform of Eqs. (24) and (25). However, as noted in Ref. 61 the validity of the noise spectrum formulation with the polaron transformation treatment is ambiguous and it can easily produce nonphysical results. Figure 3 show the spectral density with both no coupling [solid (red) line] and weak coupling for two different vibrational frequencies ω_m [$\omega_m = 1$, long-dashed (black) line; $\omega_m = 2$, long-dashed (blue) line] for $T_c = 0.2$, $\Gamma_L = \Gamma_R = 0.1$, and $N = 0.05$. There is a clear large resonance from the bare Rabi oscillations of the electron tunneling between molecules at $\omega = 2T_c = 0.4$, as well as additional resonances at $\omega = \omega_m$.
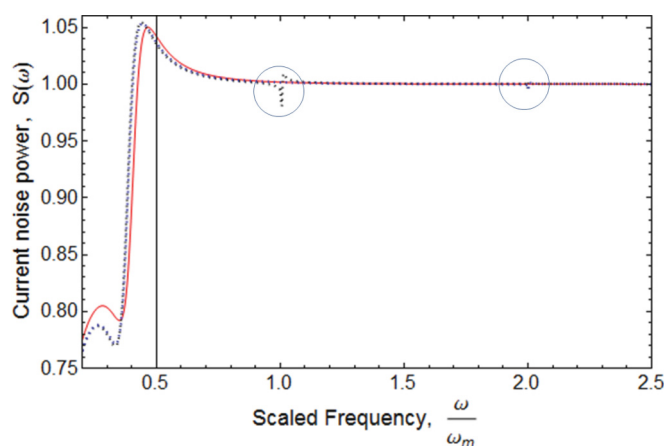

FIG. 3. (Color online) Current-noise power Fano factor $F_R(\omega) = S_R(\omega)/2eI_R$, for $\Gamma_L = \Gamma_R = 0.1$, $T_c = 0.1$, $z = 0, 0.3$, and $\omega_m = 1, 2$, and $N = 0.05$. There are two resonances, $\omega = 2T_c$ and $\omega = \omega_m$, as well as an additional higher resonance at $2\omega_m$. The latter two resonances are indicated by the two large (blue) circles.

VI. NUMERICAL COMPARISON: EXACT SOLUTION AND THE HIERARCHY EQUATION

For a small thermal occupation N and a reasonable coupling strength z and by the inclusion of damping of the vibrational mode (or an effective multimode environment), we can solve the molecule-vibration coupling exactly with a variety of different numerical approaches. Here we use the Hierarchy equation of motion for a Lorentz bath spectral density recently introduced by Ma *et al.*[64] Essentially, we take our original equation of motion but write the interaction with the vibrational mode as a bath of oscillators. We then assume that this bath has a Lorentz spectrum,

$$J(\omega) = \frac{1}{\pi} \frac{\lambda \gamma}{(\omega - \omega_m)^2 + \gamma^2}, \tag{38}$$

where λ is equal to the square of the molecule-vibron coupling strength $\lambda = g^2$, ω_m is the fundamental frequency of the vibronic excitation, and γ is the broadening or damping of the vibronic mode. We then follow the steps in Ref. 64 to reach the following hierarchical equation of motion (again setting $\hbar = 1$):

$$\frac{\partial}{\partial t} \rho_{\vec{n}}(t) = -(\mathcal{L} + n \cdot \mu) \rho_{\vec{n}}(t) - i \sum_{k=1}^{2} V^{\times} \rho_{\vec{n} + \vec{e}_k}(t)$$

$$- i \frac{\lambda}{2} \sum_{k=1}^{2} n_k [V^{\times} + (-1)^k V^0] \rho_{\vec{n} - \vec{e}_k}(t). \tag{39}$$

The superoperator notation introduced in this equation is $V^{\times} \bullet = [V, \bullet]$ and $V^0 \bullet = \{V, \bullet\}$, where V is the electronic operator that describes the coupling to the Lorentz bath, which in this case is $V = n_L - n_R$. Here, $\vec{n}$ is a two-dimensional index with positive-integer elements identifying both the true system density matrix $\rho_{(0,0)}$ and the auxiliary operators which encode the effect of the bath $\rho_{(>0,>0)}$. The other vectors are defined as $\vec{e}_1 = (1,0)$, $\vec{e}_2 = (0,1)$, and $\vec{\mu} = (\gamma - i\omega_0, \gamma + i\omega_0)$. $\mathcal{L}$ is the superoperator describing the coherent and incoherent dynamics of the molecule transport. Note that, again, here we assume a large double-occupation repulsion (Coulomb blockade), so that the electronic and transport properties are simply described by the single-electron-occupation projectors, $n_L = |L\rangle\langle L|$, $n_R = |R\rangle\langle R|$, $s = |L\rangle\langle R|$, and

$$\mathcal{L}[\bullet] = -i \left[\frac{\epsilon}{2}(n_L - n_R) + T_c(s + s^{\dagger}), \bullet \right]$$

$$- \frac{\Gamma_L}{2} D[S_L] - \frac{\Gamma_R}{2} D[S_R^{\dagger}], \tag{40}$$

where $S_L = |0\rangle\langle L|$, $S_R = |0\rangle\langle R|$, and $\mathcal{D}$ is as defined in Eqs. (19) and (20).

The tier of the hierarchy in this method must be truncated at some reasonable value, $\vec{n} = (N_c, N_c)$. Typically this is done by increasing N_c until convergence is found. If λ is increased or γ is decreased, the N_c necessary for convergence rises (representing the increased occupation of the bath and the increase in the associated degrees of freedom). The hierarchical equations of motion are solved by setting $\rho_{(0,0)}$ to the desired molecule initial state, setting all auxiliary density matrices to zero, $\rho_{(>0,>0)} = 0$, and employing direct numerical integration. Here we are primarily interested in steady-state
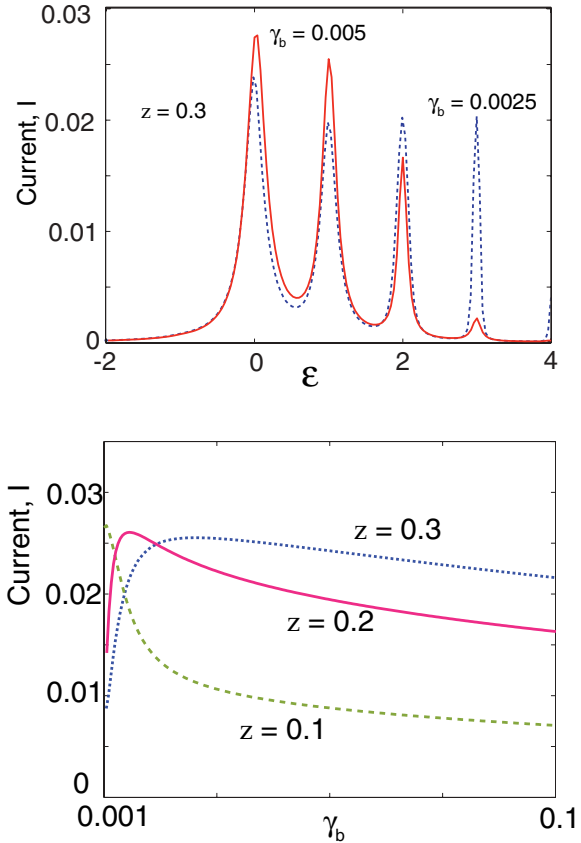

FIG. 4. (Color online) (Top) The current I_R/e as given by the exact numerical treatment for $z = 0.3$. The solid (red) curve is for $\gamma_b = 0.005$ and the dashed (blue) curve is for $\gamma_b = 0.0025$. We find that as we reduce the vibrational mode, damping current qualitatively behaves like the polaron treatment results. However, this is an additional overall reduction in magnitude not predicted by the polaron results. (Bottom) The current I_R/e as a function of damping for $\epsilon = \omega_m$, for three values of coupling strength. We see that the three curves have similar maxima but are suppressed when γ_b is reduced (the $z = 0.1$ curve is also suppressed for $\gamma_b < 0.001$).

results so we integrate until the system probabilities become stationary. The steady state can also be found by finding the null vector of the matrix defining these equations of motion.

To check the validity of this method we also directly diagonalize the equation of motion (without the polaron transform and with an additional Lindblad damping of the vibrational mode with rate $\gamma_b = \gamma/2$ in the Fock basis and integrate the resulting coupled equations of motion. We find that, given convergence, the results for the two numerical methods in the steady state match exactly. Comparing to the polaron results we see some similarities and some differences. In the top plot in Fig. 4 we see that the numerics, like the polaron treatment, predict equal height emission peaks for the different resonances as γ_b becomes small. However, as γ_b is decreased further there is also a reduction in the overall current magnitude. This is an additional localization of the electron due to the strong coupling to the vibration not captured by the polaron treatment. This phenomenon is more

clearly shown in the bottom plot in Fig. 4, where we show the current versus the vibrational mode damping at the first resonance peak, $\epsilon = \omega_m$. We see that for all coupling strengths there is a common maxima following by a suppression of the current as γ_b is reduced. This indicates that, for the purpose of current enhancement, there is an optimal finite vibrational mode damping.

In addition, the back-action lifts the off-resonance blockade seen in the polaron treatment, resulting in a finite-leakage current. For the parameters we investigate here, this does not strongly affect the notion of using this kind of device as a sensitive transistor because the contrast in the current between on- and off-resonance remains high. However, in practice there may also be additional mechanisms which decrease this contrast. Possibilities include cotunneling and dissipation channels, which may mask the resonance features.

VII. CONCLUSION

In conclusion, we have analyzed the properties of coherent electron transport through a dimer that is strongly coupled to a vibrational mode. When the energy difference between the electronic states in the two sites of the dimer is larger than the tunneling coupling, the current is suppressed. On the other hand, a semianalytical polaron treatment suggests that, when this energy difference is near the vibrational resonant frequency, an enhancement of the electron transport appears as extremely sharp and equal-height current resonances. This strong coupling also induces Frank-Condon blockade, suppressing the current between the resonances. The vibrational mode temperature determines the nature of the phonon-assisted transport. At low temperatures, phonon-emission-assisted electron transport is the dominant feature. As the temperature is increased, phonon-absorption-assisted electron transport also starts to play a role.

We also examined two exact numerical treatments of the same system. These two treatments were found to be identical in the steady state and qualitatively agreed with the polaron treatment. In addition, these results suggest that an additional localization or current suppression mechanism appears for very low vibrational mode damping, and thus there exists an optimal finite damping.

Our investigation is primarily motivated by studies of electron transport through single molecules. However, our analysis is also applicable to artificial systems, in particular, quantum dots in carbon nanotubes, where strong coupling can occur. The connection to large systems like doubly clamped semiconductor beams and cantilevers is more tenuous, as in those cases we expect the coupling to be weak and thermal phonon effects to dominate the transport properties.

APPENDIX A: BOSON CORRELATION FUNCTIONS

Here we show how to derive the analytical form for the correlation function of a single undamped oscillator mode. This is equivalent to a recent derivation given in Ref. 60. We start with a similarity transformation,

$$e^{-M} f\left(\hat{A}\right) e^M = e^{-M} \left(\sum_{n=0}^{\infty} a_n \hat{A} \right) e^M$$
$$= \sum_{n=0}^{\infty} a_n e^{-M} \hat{A} e^M = \sum_{n=0}^{\infty} a_n \tilde{A} = f\left(\tilde{A}\right),$$
(41)

which suggests that one needs to consider only the transformation on each operator separately. Utilizing the interaction picture of the boson operators and their commutation,

$$[-z\hat{b}^{\dagger} e^{i\omega t}, z\hat{b} e^{-i\omega t}] = z^2,$$
(42)

the $X(t)$ and $X^{\dagger}(t)$ operators become

$$X(t) = \exp[-z(\hat{b}^{\dagger} e^{i\omega t} - \hat{b} e^{-i\omega t})]$$
$$= \exp(-z\hat{b}^{\dagger} e^{i\omega t}) \exp(z\hat{b} e^{-i\omega t})$$
$$\times \exp\left(-\tfrac{1}{2}[z\hat{b}^{\dagger} e^{-i\omega t}, z\hat{b} e^{-i\omega t}] \right)$$
$$= \exp -z\hat{b}^{\dagger} e^{i\omega t} \exp z\hat{b} e^{-i\omega t} e^{-\frac{1}{2}z^2},$$
(43)

$$X^{\dagger}(t) = e^{-\frac{1}{2}z^2} \exp(z\hat{b}^{\dagger} e^{i\omega t}) \exp(-z\hat{b} e^{-i\omega t}),$$
(44)

then $X_t X_{t'}^{\dagger}$ becomes

$$X_t X_{t'}^{\dagger} = e^{-z^2} e^{-z\hat{b}^{\dagger} e^{i\omega t}} \left(e^{z\hat{b} e^{-i\omega t}} e^{z\hat{b}^{\dagger} e^{i\omega t'}} \right) e^{-z\hat{b} e^{-i\omega t'}}.$$
(45)

Putting the operators in normal order by using

$$e^{iH_T t/\hbar} \mathcal{O} e^{-iH_T t/\hbar} = \mathcal{O} + \left[\frac{i}{\hbar} t H_T, \mathcal{O} \right]$$
$$+ \frac{1}{2!} \left[\frac{i}{\hbar} t H_T, \left[\frac{i}{\hbar} t H_T, \mathcal{O} \right] \right] + \cdots$$
(46)

and after noting that $e^{-M} f(\hat{A}) e^M = e^{-z\hat{b}_{t'}^{\dagger}} e^{z\hat{b}_t} e^{z\hat{b}_{t'}^{\dagger}}$, with $f(\hat{A}) = e^{z\hat{b}_t}$, $\hat{A} = z e^{-i\omega t} \hat{b}$,

$$e^{-z\hat{b}_{t'}^{\dagger}} (\hat{b} e^{-i\omega t}) e^{z\hat{b}_{t'}^{\dagger}} = e^{-i\omega t} (b + z e^{i\omega t'})$$
$$\Rightarrow e^{-z\hat{b}_{t'}^{\dagger}} e^{z\hat{b}_t} e^{z\hat{b}_{t'}^{\dagger}} = e^{z e^{-i\omega t} b} \exp[z^2 e^{-i\omega(t-t')}],$$
(47)

so that

$$e^{z\hat{b}_t} e^{z\hat{b}_{t'}^{\dagger}} = \exp[z^2 e^{-i\omega(t-t')}] e^{z\hat{b}^{\dagger} e^{i\omega t'}} e^{z e^{-i\omega t} b},$$
(48)

and we obtain

$$X_t X_{t'}^{\dagger} = \exp[-z^2(1 - e^{-i\omega(t-t')})] \exp[z\hat{b}^{\dagger} (e^{i\omega t'} - e^{i\omega t})]$$
$$\times \exp[-zb(e^{-i\omega t'} - e^{-i\omega t})].$$
(49)

The correlation $\mathcal{F}$ can be arranged in a more convenient form:

$$\mathcal{F} = (1 - e^{-\beta\omega_B}) \sum_{n=0}^{\infty} \langle n | e^{-\beta n \omega_B} X_t X_{t'}^{\dagger} | n \rangle$$
$$= (1 - e^{-\beta\omega_B}) e^{-z^2(1 - e^{-i\omega_B(t-t')})}$$
$$\times \sum_{n=0}^{\infty} \langle n | e^{-\beta n \omega_B} e^{z\hat{b}^{\dagger} (e^{i\omega t'} - e^{i\omega t})} e^{-zb(e^{-i\omega t'} - e^{-i\omega t})} | n \rangle. \quad (50)$$

Let $u = z(e^{-i\omega t'} - e^{-i\omega t})$, $u^* = z(e^{i\omega t'} - e^{i\omega t})$, and expanding the exponents in a power series and using the property of destruction operators will condense the form to the Laguerre polynomial or order n:

$$\langle n|e^{u^*\hat{b}^\dagger} e^{-u\hat{b}}|n\rangle = \sum_{l=0}^{n} \frac{(-1)^l}{(l!)^2} \frac{n!}{(n-l)!}(|u|^2)^l = L_n(|u|^2). \quad (51)$$

Using one of its generating functions $\sum_{n=0} L_n\left(|u|^2\right)\xi^n = e^{-N|u|^2}/(1-\xi)$ gives

$$\mathcal{F}(\tau) = \exp\{-z^2[(1+N)(1-e^{-i\omega\tau}) + N(1-e^{i\omega\tau})]\}, \quad (52)$$

where $\tau = t - t'$. This form is still not easy to evaluate in the integral form of Eq. (27). Therefore, we expand the exponential part of Eq. (52) in terms of $\exp \pm i\omega\tau$:

$$\mathcal{F}(\tau) = e^{-z^2(1+2N)} \sum_{s,p=0}^{\infty} (z^2)^{s+p} \frac{N^s (1+N)^p}{s!p!} e^{i(s-p)\omega\tau}. \quad (53)$$

Physically, the s terms account for absorption and p for emission of phonons[60] with frequency ω. Writing

$$n = p - s = n_{\text{emit}} - n_{\text{ab}}, \quad (54)$$
$$p = s + n, \quad (55)$$

we can rewrite

$$\mathcal{F}(\tau) = \sum_{n=-\infty}^{\infty} \exp -in\omega\tau \exp -z^2 (1+2N) \left(\frac{1+N}{N}\right)^{\frac{n}{2}}$$
$$\times I_n(2z^2\sqrt{N(1+N)}), \quad (56)$$

where I_n is the modified Bessel function of the first kind. This form can be numerically evaluated. Similarly, the other correlation functions are

$$\langle X_{t'}^\dagger X_t\rangle = \langle X_{t'} X_t^\dagger\rangle = \mathcal{F}^*(\tau), \quad (57)$$
$$\langle X_t^\dagger X_{t'}\rangle = \mathcal{F}(\tau). \quad (58)$$

APPENDIX B: EQUATIONS OF MOTION FOR THE COULOMB BLOCKADE LIMIT

To obtain the analytical and numerical results we show in the second half of this work, we imposed an additional condition on our model, that of strong Coulomb repulsion against double occupation of the dimer. In this case we replace the operators with projectors onto a single-electron basis and obtain the following slightly altered equations of motion:

$$\langle \hat{n}_L\rangle_t - \langle \hat{n}_L\rangle_0 = -\frac{i}{\hbar} \int_0^t dt'[T_c(\langle \tilde{s}(t)\rangle - \langle \tilde{s}^\dagger(t)\rangle) + \Gamma_L(1 - \langle n_L\rangle - \langle n_R\rangle)], \quad (59)$$

$$\langle \hat{n}_R\rangle_t - \langle \hat{n}_R\rangle_0 = \frac{i}{\hbar} \int_0^t dt'[T_c(\langle \tilde{s}(t)\rangle - \langle \tilde{s}^\dagger(t)\rangle) - \Gamma_R\langle n_R\rangle], \quad (60)$$

$$\langle \tilde{s}\rangle_t - \langle \tilde{s}\rangle_0 = -\frac{i}{\hbar} \int_0^t dt' e^{i\epsilon(t-t')}T_c$$
$$\times \{\langle n_L X_t X_{t'}^\dagger\rangle_{t'} - \langle n_R X_{t'}^\dagger X_t\rangle_{t'}\}$$
$$-\frac{\Gamma_R}{2} \int_0^t dt' e^{i\epsilon(t-t')}\langle \tilde{s}(t') X_t^\dagger X_t\rangle, \quad (61)$$

$$\langle \tilde{s}^\dagger\rangle_t - \langle \tilde{s}^\dagger\rangle_0 = -\frac{i}{\hbar} \int_0^t dt' e^{-i\epsilon(t-t')}T_c$$
$$\times \{\langle n_R X_t^\dagger X_{t'}\rangle - \langle n_L X_{t'}^\dagger X_t\rangle\}$$
$$-\frac{\Gamma_R}{2} \int_0^t dt' e^{-i\epsilon(t-t')}\langle X_{t'} X_t^\dagger \tilde{s}^\dagger(t')\rangle. \quad (62)$$

*Corresponding author: dhs18@temple.edu

[1] L. Y. Gorelik, A. Isacsson, M. V. Voinova, B. Kasemo, R. I. Shekhter, and M. Jonson, Phys. Rev. Lett. **80**, 4526 (1998).

[2] A. Erbe, R. H. Blick, A. Tilke, A. Kriele, and J. P. Kotthaus, Appl. Phys. Lett. **73**, 3751 (1998).

[3] A. Erbe, C. Weiss, W. Zwerger, and R. H. Blick, Phys. Rev. Lett. **87**, 096106 (2001).

[4] D. V. Scheible, C. Weiss, J. P. Kotthaus, and R. H. Blick, Phys. Rev. Lett. **93**, 186801 (2004).

[5] E. M. Höhberger, T. Krämer, W. Wegscheider, and R. H. Blick, Appl. Phys. Lett. **82**, 4160 (2003).

[6] E. M. Weig, R. H. Blick, T. Brandes, J. Kirschbaum, W. Wegscheider, M. Bichler, and J. P. Kotthaus, Phys. Rev. Lett. **92**, 046804 (2004).

[7] J. Koch and F. von Oppen, Phys. Rev. Lett. **94**, 206804 (2005).

[8] S. Sapmaz, P. Jarillo-Herrero, Ya. M. Blanter, C. Dekker, and H. S. J. van der Zant, Phys. Rev. Lett. **96**, 026801 (2006).

[9] N. V. Lavrik and P. G. Datskos, Appl. Phys. Lett. **82**, 2697 (2003).

[10] K. L. Ekinci, X. M. H. Huang, and M. L. Roukes, Appl. Phys. Lett. **84**, 4469 (2004).

[11] B. Lassagne, D. Garcia-Sanchez, A. Aguasca, and A. Bachtold, Nano Lett. **8**, 3735 (2008).

[12] G. Piovano, F. Cavaliere, E. Paladino, and M. Sassetti, Phys. Rev. B **83**, 245311 (2011).

[13] T. Brandes and N. Lambert, Phys. Rev. B **67**, 125323 (2003).

[14] N. Lambert and F. Nori, Phys. Rev. B **78**, 214302 (2008).

[15] J. Koch, M. E. Raikh, and F. von Oppen, Phys. Rev. Lett. **95**, 056801 (2005).

[16] J. Koch, F. von Oppen, and A. V. Andreev, Phys. Rev. B **74**, 205438 (2006).

[17] D. A. Rodrigues, J. Imbers, and A. D. Armour, Phys. Rev. Lett. **98**, 067204 (2007).

[18] M. Aspelmeyer, P. Meystre, and K. Schwab, Phys. Today **65**, 29 (2012).

[19] C. A. Regal and K. W. Lehnert, J. Phys.: Conf. Ser. **264**, 012025 (2011).

[20] F. Marquardt and S. M. Girvin, Physics **2**, 40 (2009).

[21] D. H. Santamore, A. C. Doherty, and M. C. Cross, Phys. Rev. B **70**, 144301 (2004).

[22] J. Del Nero and B. Laks, J. Mol. Model. **7**, 354 (2001).

[23] D. B. Lima and J. Del Nero, J. Comput. Theor. Nanosci. **5**, 1445 (2008).

[24] S. J. S. Silva and J. Del Nero, J. Comput. Theor. Nanosci. **6**, 490 (2009).

[25] J. M. Mativetsky, G. Pace, M. Elbing, M. A. Rampi, M. Mayor, and P. Samori, J. Am. Chem. Soc. **130**, 9192 (2008).

[26] J. M. Seminario and L. Yan, Int. J. Quantum Chem. **107**, 754 (2007).

[27] N. L. Rangel and J. M. Seminario, J. Chem. Phys. **128**, 114711 (2008).

[28] Z. Hermon, S. Caspi, and E. Ben-Jacob, Europhys. Lett. **43**, 482 (1998).

[29] D. Wei, Y. Liu, L. Cao, Y. Wang, H. Zhang, and G. Yu, Nano Lett. **8**, 1625 (2008).

[30] M. M. D. Ramos and H. M. G. Correia, Nanotechnology **19**, 375202 (2008).

[31] R. Dost, S. K. Ray, A. Das, and M. Grell, Appl. Phys. Lett. **93**, 113505 (2008).

[32] A. Rahman and M. K. Sanyal, Nanotechnology **19**, 395203 (2008).

[33] L.-Y. Hsu, Q.-R. Huang, and B.-Y. Jin, J. Phys. Chem. C **112**, 10538 (2008).

[34] A. Bandyopadhyay, R. Pati, S. Sahu, F. Peper, and D. Fujita, Nat. Phys. **6**, 369 (2010).

[35] G. Cuniberti, G. Fagas, and K. Richter (Eds.), *Introducing Molecular Electronics* (Springer, Heidelberg, 2005).

[36] K. V. Mikkelsen and M. A. Ratner, Chem. Rev. **87**, 113 (1987).

[37] D. M. Adams, L. Brus, C. E. D. Chidsey, S. Creager, C. Creutz, C. R. Kagan, P. V. Kamat, M. Lieberman, S. Lindsay, R. A. Marcus, R. M. Metzger, M. E. Michel-Beyerle, J. R. Miller, M. D. Newton, D. R. Rolison, O. Sankey, K. S. Schanze, J. Yardley, and X. Zhu, J. Phys. Chem. **107**, 6668 (2003).

[38] Y. A. Berlin, F. C. Grozema, L. D. A. Siebbeles, and M. A. Ratner, J. Phys. Chem. C **112**, 10988 (2008).

[39] A. Aviram and M. A. Ratner, Chem. Phys. Lett. **29**, 277 (1974).

[40] T. Förster, Disc. Faraday Soc. **27**, 7 (1959).

[41] D. L. Dexter, J. Chem. Phys. **21**, 836 (1953).

[42] S. Jang, Y. J. Jung, and R. J. Silbey, Chem. Phys. **275**, 319 (2002).

[43] S. Jang, M. D. Newton, and R. J. Silbey, Phys. Rev. Lett. **92**, 218301 (2004).

[44] G. D. Scholes, J. Phys. Chem. Lett. **1**, 2 (2010).

[45] S. Jang, J. Chem. Phys. **131**, 164101 (2009).

[46] G. S. Engel, T. R. Calhoun, E. L. Read, T.-K. Ahn, T. Mančal, Y.-C. Cheng, R. E. Blankenship, and G. R. Fleming, Nature **446**, 782 (2007).

[47] G. Panitchayangkoon, D. Hayes, K. A. Fransted, J. R. Carama, E. Harel, J. Wen, R. E. Blankenship, and G. S. Engel, Proc. Natl. Acad. Sci. USA **107**, 12766 (2010).

[48] E. Collini, C. Y. Wong, K. E. Wilk, P. M. G. Curmi, P. Brumer, and G. D. Scholes, Nature **463**, 644 (2010).

[49] N. Christensson, H. F. Kauffmann, T. Pullerits, and T. Mančal, J. Phys. Chem. B **116**, 7449 (2012).

[50] T. Mančal, N. Christensson, V. Lukeš, F. Milota, O. Bixner, H. F. Kauffmann, and J. Hauer, J. Phys. Chem. Lett. **3**, 1497 (2012).

[51] J. G. Müller, U. Lemmer, G. Raschke, M. Anni, U. Scherf, J. M. Lupton, and J. Feldmann, Phys. Rev. Lett. **91**, 267403 (2003).

[52] D. J. Heijs, V. A. Malyshev, and J. Knoester, Phys. Rev. Lett. **95**, 177402 (2005).

[53] M. H. Chang, M. J. Frampton, H. L. Anderson, and L. M. Herz, Phys. Rev. Lett. **98**, 027402 (2007).

[54] I. Yamazaki, S. Akimoto, T. Yamazaki, S. Sato, and Y. Sakata, J. Phys. Chem. A **106**, 2122 (2002).

[55] K. Gaab and C. J. Bardeen, J. Phys. Chem. B **108**, 4619 (2004).

[56] N. Ogawa, A. Miyata, H. Tamaru, T. Suzuki, T. Shimada, T. Hasegawa, K. Saiki, and K. Miyano, Chem. Phys. Lett. **450**, 335 (2008).

[57] J. Gilmore and R. H. McKenzie, Chem. Phys. Lett. **421**, 266 (2006).

[58] A. J. Leggett, S. Chakravarty, A. T. Dorsey, M. P. A. Fisher, A. Garg, and W. Zwerger, Rev. Mod. Phys. **59**, 1 (1987).

[59] H. Dekker, Phys. Rev. A **35**, 1436 (1987).

[60] G. Schaller, T. Krause, T. Brandes, and M. Esposito, arXiv:1206.3960.

[61] T. Brandes, Phys. Rep. **408**, 315 (2005).

[62] L. A. Pachón and P. Brumer, J. Phys. Chem. Lett. **2**, 2728 (2012).

[63] S. Jang, Y.-C. Cheng, D. R. Reichman, and J. D. Eaves, J. Chem. Phys. **129**, 101104 (2008).

[64] J. Ma, Z. Sun, X. Wang, and F. Nori, Phys. Rev. A **85**, 062323 (2012).

[65] Y. Tanimura, Phys. Rev. A **41**, 6676 (1990).

[66] J. Stettenheim, M. Thalakulam, F. Pan, M. Bal, Z. Ji, W. Xue, L. Pfeiffer, K. W. West, M. P. Blencowe, and A. J. Rimberg, Nature **466**, 86 (2010).

[67] M. Bockrath, D. H. Cobden, P. L. McEuen, N. G. Chopra, A. Zettl, A. Thess, and R. E. Smalley, Science **275**, 1922 (1997).

[68] B. Lassagne, Y. Tarakanov, J. Kinaret, D. Garcia-Sanchez, and A. Bachtold, Science **325**, 1107 (2009).

[69] G. A. Steele, A. K. Hüttel, B. Witkamp, M. Poot, H. B. Meerwaldt, L. P. Kouwenhoven, and H. S. J. van der Zant, Science **325**, 1103 (2009).

[70] H. B. Meerwaldt, G. A. Steele, and H. S. J. van der Zant, *Fluctuating Nonlinear Oscillators* (Oxford University Press, Oxford, UK, 2012).

[71] T. Brandes, R. Aguado, and G. Platero, Phys. Rev. B **69**, 205326 (2004).

[72] R. Aguado and T. Brandes, Phys. Rev. Lett. **92**, 206601 (2004).

[73] D. K. C. MacDonald, Rep. Prog. Phys. **12**, 56 (1948).